3D MICROFABRICATED SCAFFOLDS AND MICROFLUIDIC DEVICES FOR OCULAR SURFACE REPLACEMENT: A REVIEW

Elisabetta Prina[1], Pritesh Mistry[1], Laura E. Sidney[2], Jing Yang[1], Ricky D. Wildman[3], Marina Bertolin[4], Claudia Breda[4], Barbara Ferrari[4], Vanessa Barbaro[4], Andrew Hopkinson[2], Harminder S. Dua[2], Stefano Ferrari[4,*], Felicity R. A. J. Rose[1,*]

[1] *Division of Regenerative Medicine and Cellular Therapies of Advanced Drug Delivery & Tissue Engineering, School of Pharmacy Centre for Biomolecular Sciences, University of Nottingham, Nottingham, United Kingdom*

[2] *Academic Ophthalmology, Division of Clinical Neuroscience, University of Nottingham, Nottingham, United Kingdom*

[3] *Department of Chemical and Environmental Engineering, University of Nottingham, Nottingham, United Kingdom*

[4] *Fondazione Banca degli Occhi del Veneto, Venice, Italy*

**Authors contributed equally to this work*

The authors declare no potential conflicts of interest

Corresponding author

Stefano Ferrari, PhD

Fondazione Banca degli Occhi del Veneto

c/o Padiglione G. Rama - Via Paccagnella 11

30174 Zelarino (Venezia)

ITALY

Tel.: +39 041 9656474

Fax.: +39 041 9656471

Email: stefano.ferrari@fbov.it

Abstract

In recent years, there has been increased research interest in generating corneal substitutes, either for use in the clinic or as *in vitro* corneal models. The advancement of 3D microfabrication technologies has allowed the reconstruction of the native microarchitecture that controls epithelial cell adhesion, migration and differentiation. In addition, such technology has allowed the inclusion of a dynamic fluid flow that better mimics the physiology of the native cornea. We review the latest innovative products in development in this field, from 3D microfabricated hydrogels to microfluidic devices.

Keywords

Cornea, topography, microfabrication, 3D model, microfluidics

Introduction

There is a growing clinical need for corneal grafts for use in corneal transplantation. Each year the prevalence of patients requiring corneal transplants increases, and currently only 1 in 70 cases are treated [1]. The disparity is worse in the developing parts of the world where prevalence of corneal blindness is greater. Donor grafts can vary in quality and may be rejected by the host immune system [2, 3, 4]. Eye banks are unable to meet the demand and therefore an alternative source is required. Bioengineered corneal replacements can potentially overcome this shortage by providing tailored scaffolds with the inclusion of cells from the patient to minimize the risk of rejection. These substitutes can be used, not only as biomimetic corneal equivalents for use in transplantation, but also to study corneal pathologies *in vitro*. In recent years, several studies have focused on recreating the complex dynamic microenvironment and here we have classified these studies into three categories: topography, microarchitecture, 3D co-culture and microscale flow (Fig. 1). The final section of this review focuses on innovative additive manufacturing technologies, and how they could be used to develop cornea substitutes in the near future.

Physiology of the cornea and clinical issues

The cornea is a transparent window at the front of the eye, and is primarily responsible for focusing light onto the retina. It accounts for two thirds of the focusing of light, the remainder being achieved by the crystalline lens. The cornea is composed of five major layers: the epithelium, Bowman's layer, stroma, Descemet's membrane and the endothelium. A sixth layer, Dua's layer, situated at the posterior stroma, was postulated in 2013 [5]. At the anterior cornea, facing the outside environment, is the epithelium, a stratified cellular layer composed of non-keratinized squamous epithelial cells bathed by the tear film, which gives it its final optical polish. The original source of these epithelial cells is the limbal epithelial crypts, a stem cell niche found in the outer ring of the cornea [6, 7]. These limbal stem cells allow the epithelium to self-renew and heal defects. The replacement of these cells has been most successful through regenerative medicine therapies. If a patient has limbal stem cell deficiency, or if the limbus is missing, a limbal stem cell transplant can be performed [8]. The first stem cell-based product to receive a marketing authorization (even if conditional) by the European Medicines Agency was Holoclar (Chiesi Farmaceutici SpA), an *ex vivo* cultured autologous limbal stem cell graft. However, this treatment is only currently available in Europe, where it can be used to treat patients with severe corneal burns.

Separating the epithelium from the stroma below is the Bowman's layer, a tough acellular layer composed predominantly of collagen and laminin. The middle layer of the cornea, the stroma, makes up the bulk of the thickness of the cornea, and consists primarily of lamellar sheets of collagen-I fibrils arranged in a highly-ordered manner compatible with corneal transparency. The stroma is populated with cells of mesenchymal origin called keratocytes, responsible for maintaining the structured extracellular matrix (ECM) of collagen and proteoglycans [9–12]. In a healthy cornea, keratocytes exhibit a dendritic morphology, with extensive cellular contacts [13, 14]. However during trauma or disease these cells can become activated and exhibit morphological characteristics of fibroblasts and commence tissue remodelling [15, 16]. In later stages of remodelling, a myofibroblast phenotype also appears, expressing α-smooth muscle actin (α-SMA). This can cause scar formation, contraction and loss of corneal transparency [14, 17, 18]. Evidence has been presented demonstrating that the limbal region of the corneal stroma also contains a mesenchymal stem cell population that can be used to regenerate the cornea [19, 20].

The posterior two layers of the cornea are the Descemet's membrane, a thin acellular layer composed mainly of collagen-IV, which acts as a modified basement membrane for the final layer, the corneal endothelium. The corneal endothelium is composed of simple cuboidal cells that maintain fluid balance within the cornea. These cells are not related to vascular or lymphatic endothelial cells. Corneal endothelial cells have very limited proliferative capacity *in vivo*, dividing rarely in the adult cornea [21, 22]. As a result, wounding and trauma of the endothelium is difficult to reverse. A relatively increased concentration of elastin has been shown to run as an annulus along the limbus in the peripheral cornea and in the pre-Descemet's layer (Dua's layer) [23].

Worldwide, corneal disease is the second most prevalent cause of blindness after cataracts [24]. Corneal blindness is considered avoidable and treatable in many cases, as corneal transplantation surgery can be performed. However, there is a current global shortage of donor corneas and, in many developing countries, there is no dedicated and funded eye bank facility to procure corneas. Based on data from the World Health Organisation, it is estimated that at least 4 million people worldwide suffer from corneal blindness. However, only 100,000 corneal transplants are performed each year, primarily as a result of lack of access to suitable tissue. The majority (90%) of the global cases of ocular trauma and corneal ulceration leading to corneal blindness occur in developing countries

[24]. The incidence of corneal blindness in India is 25,000-30,000 every year with a prevalence of approximately 6.8 million people who have visual acuity less than 6/60 in at least one eye due to corneal diseases [25].

For most people, corneal transplantation can restore vision with a 5 year graft survival rate of 74%. However, 1 in 6 full thickness transplants still experience some degree of rejection, predominantly due to the variable quality in the donor tissue's endothelial or epithelial health. In patients with alkali burns or recurrent graft failures, the chance of transplantation success is lowered considerably [26]. These issues with donor cornea shortage and rejection indicate that there is a need for new, innovative therapies to be developed that can be used to treat corneal blindness worldwide.

Topography

The geometric patterns on the surface of a culture substrate, referred to as the topography, induces cells to align or orient themselves along specific features. In addition, the topography can impact cell physiological functions by inducing changes in cell proliferation, migration, differentiation, and by controlling cell homeostasis. The effect of surface topography on cell behaviour, known as contact guidance, is very well known, but only in the last few years, research has focused on its development at the nanoscale thanks to advances in manufacturing techniques. One method that has been used to produce topographical features is lithography, a technique by which 2D patterns with high fidelity and excellent resolution can be fabricated. Topography has been used to study cell interactions with different surface patterns, and has been used to guide cell-extracellular matrix interactions [27–31].

In the central cornea, epithelial cells adhere to the underlying stromal layer via a basement membrane whose topography displays a characteristic nanoscale architecture (20-400 nm). Described as "felt-like", the mountainous surface varies in height, pore size and fibre diameter [32]. The function of this layer is still unclear, but it may influence cell behaviour. Using atomic force microscopy and scanning electron microscopy techniques, the height of the elevations, pore diameters and fibre diameters were found to be in the ranges of 47-380 nm, 30-191 nm and 22-92 nm, respectively (Fig. 2A).

Teixeira and colleagues have investigated the impact of nano- and microscale features on human corneal epithelial cell (hCEC) behaviour [33–35]. Six patterns of grooves and ridges were produced; pitch dimensions ranged from

400 nm (70 nm ridge width) to 4000 nm (1900 nm ridge width), with a depth of 600 nm (Fig. 2B). The smallest pattern investigated was within the range of dimensions found in the native basement membrane. hCECs were cultured on these surfaces in two different culture media: serum-free medium (EpiLife, Thermo Fisher Scientific) or F12 Dulbecco's Modified Eagles Medium (DMEM). They showed that cell alignment was parallel to the grooves and ridges in the microscale dimension (2000-4000 nm), independent of the cell culture medium used. However, cell response was modulated by the soluble factors in the medium when cultured on the nanoscale dimension. In serum-free media, hCECs shifted from parallel to perpendicular alignment, as feature sizes decreased from microscale (4000 nm) to nanoscale dimensions (400 nm), while in F12 DMEM, cells aligned parallel to the grooves and ridges regardless of the feature size [35]. The group hypothesised that, in addition to the topography, the transduction of cell-substrate interactions may be influenced by one of the seventeen differences found between the compositions of the media. To evaluate the lower limit in substratum feature dimensions in which hCECs exhibit contact guidance, Tocce et al. prepared wave-like ridge and groove features smaller than 400 nm (70 nm ridge width). Patterns, with pitches of 60, 90 and 140 nm (30, 45, 70 nm ridge widths, respectively, and 200 nm depth) were produced, mimicking the lower range of dimensions observed in the basement membrane. In addition, to study the combined effect of nano- and microscale features, 70 nm ridges were overlaid on a microscale topography (400-4000 nm). The minimum pitch dimensions in which cells displayed contact guidance were 60 nm and 90 nm, when cells were cultured in EpiLife and in epithelial medium (containing Ham's F12, and DMEM, supplemented with foetal bovine serum, hydrocortisone, cholera toxin, insulin, adenine, and epidermal growth factor), respectively. Nevertheless, the percentage of cells that were aligned was only 15% in these conditions, but increased to 50% at 90 nm and 20% at 140 nm, in EpiLife and epithelial medium, respectively. Interestingly, when the 70 nm pitch was overlaid on 4000 nm grooves and ridges, there was an increase in the cell alignment, in comparison to either pitch alone [36]. Yet, it would have been interesting to see if this phenomenon had been observed using EpiLife media. This suggests that the combined effect of nano- and macroscale topography can have an influence on cell alignment, even in the range where nanoscale features do not show any obvious effect. In addition, cell alignment is also influenced by the depth of the patterns, a factor which should be considered [37, 38].

Eberwein et al. examined the effect of micro-pillars on the morphogenesis, proliferation and differentiation of immortalized cornea epithelial cells, referred to by the authors as keratinocytes [39]. Micro-pillars, each 15 µm in height and 5 µm in width, were printed onto PDMS with variable spacing (5, 7, 9, and 11 µm). The tops of the pillars were biofunctionalised with fibronectin to confine cell adhesion to these areas. Immortalized human corneal keratinocytes demonstrated flattened morphology on 5 µm arrays, whereas on 11 µm arrays, cell morphology was more rounded. Proliferation appeared to be attenuated at 11 µm, with a lower metabolic activity in comparison to 5 µm spacing. Differentiation was more pronounced at 11 µm, with a higher expression of late differentiation markers (keratin 12) and terminal cornea differentiation (involucrin and filaggrin), and lower expression of early differentiation markers (keratin 19), compared to 5 µm spacing. Curiously, the level of stem cell marker (ABCG2) also increased on the 11 µm feature. Although the article points out that the mechanism underpinning this behaviour may be related to the increased stressful environment, which encourages differentiation by facilitating their survival under stress, it would have been interesting to compare the results with a flat (no pillar) surface.

Similar to corneal epithelial cells, topography has also been shown to influence corneal endothelial cells. In their native environment, the basal surface of corneal endothelium is in contact with Descemet's membrane, a layer consisting of nanoscale fibres and pores [32]. Yim and colleagues studied the impact of micro- and nanoscale topographies of different geometries [40], and the combined effect of topography with ECM coatings [41]. In the paper by Koo et al., nano-pillar structures (250 nm diameter, 250 nm height, 500 nm pitch), micro-wells (1 µm diameter, 1 µm depth, 6.7 µm pitch) and micro-pillars (1 µm diameter, 1 µm height, 6.7 µm pitch) were investigated [41]. Three biochemical cues (fibronectin-collagen I, a fibronectin collagen mix (FNC Coating Mix®; US Biological) and laminin-chondroitin sulfate) were examined and supplemented in the form of ECM protein coatings on the PDMS substrates. Similar to the epithelial behaviour, the combined effect of topography and biochemical cues modulated human corneal endothelial cell line morphometry and phenotype. For example, the combination of fibronectin coating with 1 µm pillars displayed enhanced gene and protein expression of Na^+K^+-ATPase and junction-associated protein Zona Occludens 1 (ZO-1) (significant markers for cornea endothelium function), the highest circularity, and the smallest cell area (a factor relating to the maintenance of polygonal morphology), when

compared to other patterns and the unpatterned control. Nevertheless, neither the patterns nor the coatings showed a specific trend with respect to the unpatterned surface.

Overall, the literature suggests that micro- and nanoscale topographical features, in combination with soluble factors, control corneal epithelial and endothelial behaviour. For this reason, the incorporation of these patterns should be considered to improve the design of scaffolds for corneal tissue engineering. Nevertheless, in the majority of the previously described studies, cells were generally seeded on a silicon wafer or biomaterials that cannot be used in tissue engineering applications, as they are unable to integrate with the host milieu. In this perspective, it is necessary to recreate and investigate topographical features by using biomimetic materials suitable for cornea transplantation, and in addition, such studies must examine the collective migration of cells opposed to single cell migration. Photolithography, soft lithography, and microcontact printing are common techniques used to produce topography on biocompatible materials. Lawrence et al. investigated the effect of lined patterned biomimetic silk films (2 μm width and 4 μm pitch) on collective cell migration, using an immortalized human corneal-limbal epithelial cell line [42]. The use of silk allowed for optical transparency to be achieved and it has already been used to support limbal epithelial cell and mesenchymal stroma cell growth [43]. The group found that the migratory direction of individual cells and a collective epithelial sheet was influenced by the underlying topography. The migration rate was higher in the parallel compared to the perpendicular direction. On the contrary, migration was isotopic on the flat silk. Both, the use of serum-free media, and the pattern dimensions were comparable to the work by Teixeira et al. [34], showing that the individual and collective cell migration was guided by the topography. Further research investigated the use of soft lithography on silk films to replicate corneal stromal tissue architecture [44–46].

Topographic features were also incorporated by replica-moulding onto RGD-functionalized PEGDA. Three different topological features were prepared (grooves and ridges with either 400, 1400 or 4000 nm pitches) and human corneal epithelial cell proliferation and migration were evaluated using a modified wound healing assay [47]. The patterned surfaces exhibited a 50% enhancement in the rate of corneal epithelial wound closure, compared to flat surfaces with the same chemical composition. Although isolated cells aligned parallel to the topography, confirming

the aforementioned results, no contact guide was exhibited by cells on the border of the wound. Active migration at the wound edge and an increase in the expression of cell migration marker laminin-332 were found on the topographic substrate [47]. In a further study, collagen-based micropatterned films were studied. The collagen, moulded with grooves 30 µm in depth, 10 µm in width and 2 µm in ridge width, was chemically crosslinked for stability. Although the dimensions investigated differ from the aforementioned articles, the human cornea keratocytes showed an orientation parallel to the grooves. However after reaching confluence, the cells adhered to the inclined walls, and after three weeks the cell pattern was no longer observed [48]. Topography has also been incorporated on a hydrogel composed from interpenetrating networks of recombinant human collagen type III and 2-methacryloyloxyethyl phosphorylcholine (RHCIII–MPC). This material, previously tested in animal models and in a clinical study as a corneal implant, promoted epithelial, stromal cell and nerve regeneration [49–51]. The incorporation of fibronectin patterns using a microcontact technique promoted *in vitro* cell adhesion, and a pattern of 30 µm wide strips separated by 60 µm spaces showed higher expression of Ki67, integrin β1, and focal adhesion kinase, and markers of proliferation [52]. Islam and colleagues showed that RHCIII–MPC could be precisely shaped using a femtosecond laser (developed for ophthalmic surgery) and crosslinked with riboflavin/UV *in situ*, meaning that the gel could be cut to match the exact defect as required. This technique, in combination with microscale patterns, could potentially be used to enhance the speed of host integration and, due to the perfect fit, removes the need to suture the implants [52]. This would also have the potential of building the patients' refractive correction into the gel to improve unaided vision.

In addition, the topography may have an impact on the transplantation outcomes of amniotic membrane (AM). AM is the innermost layer of three layers that together form the foetal membrane. It is composed of a layer of endothelial cells, a basement membrane and a thin connective tissue membrane. AM is widely used in ophthalmology [53] as substrate for limbal epithelial stem cell expansion due to its ability to preserve limbal stemness *in vitro* [54], and the epithelium has been found to contain a number of biological factors and proteins [55]. However, inter- and intra-sample variation can cause unpredictable outcomes (reviewed at [56]). Beyond mechanical properties [57], AM variation may be associated with the heterogeneity in the surface topography, which is responsible for controlling the differentiation process. It has been demonstrated that increasing the surface roughness from 3.4 to 13.1 nm, the gene expression of stem markers p63 and ABCG2, and protein expression of

ABCG2 increases [58], confirming the previous results reviewed above. Modification of the nanotopography was achieved by increasing the time (0-4 hours) in which the AM was immersed in the crosslinking solution (1-ethyl-3-(3-dimethyl aminopropyl) carbodiimide (EDC) and N-hydroxysuccinimide (NHS)). Furthermore Ma and colleagues have showed that, when used as an epithelial basement membrane (EBM)-like substrate, carbodiimide-crosslinked denuded AM (CLDAM) was a better substrate than denuded AM for preserving human limbal epithelial stem cells (hLESCs) *in vitro* [59]. The group used this material to study the underlying mechanism of hLESCs homeostasis and found that cultures on CLDAM displayed greater expression of p63, ABCG2, integrin β1 and integrin-linked kinase (ILK), the latter of which was also found to be an important mediator in signal transduction. Their data suggests that signals are transduced from integrin β1 to the master gene in hLESCs regulation, deltaNp63α, via ILK and the Wnt/β-catenin pathway, and that these signals are dictated by the roughness of the EBM substrate.

The importance of surface pattern was recently exploited by Wang et al [60], developing a complex 3D model that included patterned silk as a guidance for human epithelial, stromal and neuronal cells, depicted in Fig. 3. Silk films, either stamped or patterned, were used as substrates for human epithelial cells and human stromal cells, respectively; the latter were differentiated into keratocytes. Epithelial layers were cultured upon stromal cell layers, and both were surrounded by a silk sponge embedded with dorsal root ganglion cells. Different patterns of nerve growth factor (NGF) at different concentrations were loaded into the epithelial silk film to provide guidance for neuronal extensions. A collagen solution was cast on top of the film for scaffold integrity, and an air-liquid interface system was designed to enhance the maturity of the epithelium. This approach allowed the group to closely mimic the corneal anatomy and could be applied in corneal physiology research. However, to achieve a self-renewing cornea representation, the incorporation of an enclosed area that mimics the stem cell niche, would be of interest. In the next section, studies related to this topic will be discussed in detail.

Microarchitecture

In the treatment of corneal pathologies, when the limbus is damaged, the preferred scaffold should support a permanent source of epithelial progenitor cells to ensure the maintenance of corneal homeostasis. Such cells, if harvested from the human cornea, will ultimately change their phenotype and lose their stemness. Stemness may be maintained, in part, by matching the architecture of the scaffold to the source niche. For example, limbal

epithelial cells outgrowing from an *ex vivo* explant on AM scaffolds progressively lose their stemness *in vitro*, as the distance from the explant increased [61]. Recently, progress in the design of corneal scaffolds has been made by the inclusion of 3D spatially defined structures that resemble limbal niches and act as stem cell reservoirs. Fig. 3 depicts techniques that have been used to produce scaffolds which incorporate these localised, enclosed architectures for tissue engineering applications. Ortega and colleagues used stereolithography to develop a poly(ethylene glycol) diacrylate (PEGDA) ring with micro-pockets (150-350 nm diameter and 80-100 μm depth) to mimic the limbal niche [62]. The addition of fibronectin, in combination with the micro-pockets, enhanced cell attachment and outward migration of rabbit limbal fibroblasts. In addition, after 6 weeks of culture, a scaffold, seeded with rabbit limbal epithelial cells, was placed onto an *ex vivo* wounded cornea model. The outgrowth of cells and the formation of a multi-layered epithelium was observed. However, only the expression of the differentiation marker cytokeratin 3 (CK3) was analysed on the PEGDA ring and was found to be expressed by the cells in the pockets.

In a further study, Ortega and colleagues combined stereolithography with electrospinning to reproduce the micro-pocket ring [63, 64]. Stereolithography was first used to fabricate a PEGDA template. Poly(lactic-co-glycolic acid) (PLGA) was then electrospun on top (Fig. 4A); the fibres adopted the shape of the microfabricated structure. This model included micro-pockets with diameters in the range of 300-500 μm. Inside the pockets, 61% of the fibres showed high alignment, whilst outside, they were randomly orientated and presented a higher fibre density. This conferred differential mechanical properties between the inside and the outside of the artificial niches, and guided rabbit epithelial cells cultured inside the pockets to migrate outwards and towards the central region of the scaffold. This method facilitated the control of the directionality of cell migration, and the control of the morphology of rabbit cornea fibroblasts and epithelial cells, both of which were more elongated inside the pockets with respect to the outside, where they were shorter and polygonal. This study, looking at the modulation of the mechanical environment between different regions could be a crucial aspect as durotaxis may stimulate corneal epithelial migration and differentiation [65]. Rabbit limbal fibroblasts were seeded on the membrane and either a rabbit limbal epithelial cell suspension or a limbal explant was placed inside the niche [64]. Regarding differentiation, expression of the putative stem cell marker p63 was detected in proximity to the explant, when placed inside the pockets. Yet, the p63 marker was not detected when a rabbit limbal epithelial cell suspension was seeded inside

the pockets, and no differences in the expression of CK3 and p63 were observed between cells inside and outside the pockets. It is unclear whether these niche structures alone are able to recreate the limbal stem cell niche *in vitro* and further investigations are required.

Another biomaterial that can be used to generate scaffolds with micro-patterns for use in tissue engineering applications is compressed collagen. Collagen is abundant in the cornea, and many groups have used this protein for fabricating scaffolds for cornea regeneration, especially for stroma applications (reviewed at [66]). A critical aspect, however, is its structural weakness. Compressed collagen, which displays improved mechanical strength with respect to its non-compressed counterpart, has been adopted for the expansion of limbal epithelial stem cells, and shows biocompatibility comparable to AM [67, 68]. This technique has already been used to control surface micro-topography of hydrogels [69] (Fig.4B). Using this technique, Levis et al. developed a Real Architecture for 3D Tissue (RAFT) system, in which microscale grooves and ridges were reproduced to simulate the structure of limbal stem cell niches [70–72]. In their model, the ridges (in the range of 100-250 μm width and depth) were localised to the external part of the scaffold, keeping the central area flat. Human limbal stromal fibroblasts were embedded in the gel and human limbal epithelial cells were seeded on the surface. After 3 weeks of culture, the constructs formed numerous epithelial layers and maintained a mixed population of primitive and differentiated cells, with a high percentage of the cells lining the base of the crypts staining positive for the limbal stem cell marker p63α [71]. Their architecture well represented the interpalisadal grooves that stretch radially towards the cornea, termed limbal crypts [73], but was less representative of the enclosed structure that, from histological analysis, is widest at the origin and gradually narrows at its termination, extending beneath the sclera in radial, circumferential and oblique directions, described as epithelial limbal crypts [7]. Further examination of this anatomical space in 2015 identified both structures: narrow, frequent radial structures as well as larger, wider crypts [74].

3D control of microscale flow

The surface of the cornea is under the constant influence of a dynamic microenvironment created by spontaneous eye blinking and the spread of the tear film, which facilitates the hydration and lubrication of the cornea and conjunctiva. Given that the volumes involved in the hydration of the cornea are in the micron scale, microfluidic devices have aided in the creation of systems that closely mimic the *in vivo* cornea environment. Microfluidics is

the study of processes and systems that are capable of controlling fluid flow, mixing and reactions in small (1-100 µm) channels. They are able to manage small volumes, which are comparable to *in vivo* tear volumes and tear flow, approximately 7±2 µl and 0.95-1.55 µl min^{-1}, respectively [75, 76].

The majority of studies combining both microfluidics and the cornea have focused on the pharmacokinetics of drug release using acellular models for a tear replenishment system [77–79], or to quantify tear proteins [80, 81]. Their aim is to replace *ex vivo* and *in vivo* animal models which often fail to model the biological response in humans, constantly face ethical issues, and to provide a more *in vivo*-like replacement for conventional *in vitro* static models. Bajgrowicz and colleagues compared drug flow release from contact lenses in static and dynamic conditions. In the conventional static model, contact lenses were immersed in cell culture media, while the dynamic model consisted of a microfluidic device where a volume of approximately 100 µl was injected to simulate the tear process. The results indicated that drugs were released more slowly and at a far more constant rate over 24 hours in the microfluidic device, whilst in the static condition, drug release occurred rapidly within the first hour [78, 79]. Furthermore, a microfluidic platform was developed by Guan et al. to build a personalized assessment of lens care solution performance [82]. This "medical device-on-a-chip" combined the microscale of tear volume (1 µl) with the macroscale of commercial contact lenses (1 mm). They developed a system in which patient tears were used to test the best cleaning solution and lens material. This prototype is an interesting approach towards personalized medicine in cornea applications, however, should be confirmed by tests performed in a larger sample.

Few groups have developed microfluidic models in combination with cells. To test the effect of tear fluid on the ocular bioavailability of topical drugs, Pretor et al. developed a model that mimicked the shear stress generated by eyelid wiping and fluid flow of tears *in vivo* [83]. This aspect is considered to be determinant in the permeation of drugs across the cornea barrier. A microchannel device (volume 15 µl), in which immortalized human corneal epithelial cell lines were inoculated after a poly-D-lysine-coating, was exposed to colloidal drug formulations and observed using a live cell imaging approach. The model was used as a drug uptake study, and static and dynamic approaches were compared. Shear stress (0.1 Pa) and a flow rate of 0.1 ml min^{-1} was applied to the cells. Cell viability was tested before and after the application of the drugs. The shear stress did not have a substantial effect on cell viability. Nevertheless, it will be interesting to investigate a range of shear stress closer to the *in vivo* value (0.03-15 Pa) [84]. Kang et al. also attempted to replicate the micro-mechanical environment of a blinking eye [85].

Three conditions were applied on rabbit limbal epithelial stem cells, using a custom-designed bioreactor: no flow (static), steady flow, and intermittent flow. The flow rate was set to 0.93 mL min^{-1}, applied for 2 hours per day (for 2 days) for steady flow and with a 1 min on/3 min off cycle for the intermittent flow. Bromodeoxyuridine staining (to assess proliferation), real-time PCR (to investigate the expression of stem cell markers Notch-1, p63 and Bmi-1, and differentiation markers K3 and K12), and immunofluorescence staining (to detect the presence of Bmi-1, K3 and K12), were conducted before (day 7) and after the application of the stimuli (day 10 and day 14). At day 14 the steady flow condition appeared to have an effect on cell proliferation and on Bmi-1 expression, whilst the intermittent flow condition induced differentiation of LESCs, via expression of K3 and K12. In general, it was demonstrated that limbal epithelial cells responded to the mechanical stimulation generated by the flow conditions, though further investigations are necessary. Although it is well known that it is possible to control cell proliferation and differentiation (reviewed at [86]) by applying shear stress, this aspect has not yet been fully investigated in limbal cells.

Puleo et al [87] increased the complexity of the system from conventional 2D culture by combining 3D tissue-like architecture with microfluidic devices. Cornea epithelial cells were seeded on one side of vitrified collagen and placed in-between a microfluidic device. After reaching confluence, a collagenase solution was injected within the basal side of the microfluidic device which enzymatically degraded the underside of the collagen. Corneal keratocytes were then seeded and cultured on the basal side of the existing epithelium. The recreation of the corneal micro-tissue bilayer allowed the group to perform transepithelial permeability tests under different growth conditions at a microscale level.

Microfluidics in cornea-related works also include platforms in which strain and electric stimulation are applied to cornea cells. Winkler et al. produced a microfabricated system that studied the impact of cyclical strain (cyclical inflate/deflate at 0.5 Hz), applied for up to 48 hours, to stretch cornea cells and to evaluate cell *de novo* collagen fibre alignment [88]. Rabbit cornea cells were seeded on a polydimethylsiloxane (PDMS) membrane coated with collagen gel. Cell and collagen fibre alignment were observed using bright-field microscopy, confocal microscopy, and nonlinear optical imaging by removing the membrane. Precise *in vivo* spatial organization of collagen I fibres is one of several factors responsible for corneal optical transparency [89, 90], including, but not limited to, fibril diameter, fibril density, and corneal thickness [91]. Another study fabricated the first electrotaxis-on-a-chip device:

a microfluidic platform for high-throughput electrotaxis studies. Although the application of an electrical field has already been tested in clinical trials for the treatment of chronic wounds (reviewed at [92]), and applied to bovine cornea epithelial cells [93] and immortalized human cornea epithelial cells [94], in combination with topographically patterned surfaces, this work included all the components for cell migration under electrical field stimulation in a miniaturize platform. Immortalized human cornea cell migration was studied under electrical field stimulation of different strengths (2.1 mV mm^{-1} to 1.6 V mm^{-1}) [95]. The results showed that directional cell migration is dependent on electrical field strength, and so this device could potentially be adopted to promote cell migration in corneal wound healing applications. In all these studies, the research has mainly focused on one specific aspect of the cornea homeostasis, and has not considered the complexity of the system.

Microfabrication technology - "tissue-like structures" - future development

In the past few years, research groups have proposed innovative methods to exploit additive manufacturing techniques for studying cell-material interaction, and to control the arrangement of cells and biomolecules in defined scaffold geometries.

Printing structures, with the specific size and shape of the target organ, which include cells from the patient or induced Pluripotent Stem Cells (iPSCs), could be used in replacement therapies to decrease the risk of rejection, which is an issue over the long term [96]. These techniques would face the problem of the limited number of donor cells available for transplantation.

These attempts aimed to recreate controlled 3D architectures, better mimicking *in vivo* 3D microenvironments and dimensions, facilitating the regenerative process, as it has been recently demonstrated for example by printing embryonic stem cells and materials in a spatially controlled manner [97].

Nevertheless, reports of additive manufacturing for eye-related applications are still scarce and mostly unexplored. Additive manufacturing, also known as 3D printing, refers to a technique in which 3D digital models are created using Computer Aided Design (CAD) software, and then manufactured by the deposition of successive layers of materials to generate 3D objects [98]. The additional complexity of 3D bioprinting in comparison to non-biological printing is given by the need to carefully select materials, cell lines, and growth factors. Although additive manufacturing comprises several techniques, the most common in the field of bioprinting are inkjet printing,

extrusion-based bioprinting, laser-assisted printing and stereolithography. Here we will discuss current techniques and how they may be applied towards cornea-related applications.

During inkjet bioprinting, droplets of liquid, often picolitre in volume, containing biological materials are delivered to specific locations on a substrate by means of thermal or acoustic forces. In thermal inkjet systems, the droplet is forced out from the nozzle by air pressure pulses generated by electronically heated elements in the print-head. In acoustic inkjet systems, the pulses are generated by ultrasound or piezoelectric actuators. Advantages of this technique are high fabrication speeds, high resolution (20–100 μm), low cost and wide availability, whilst drawbacks include both thermal and mechanical stresses, low accuracy of droplet localization, and low cell densities. The inkjet approach has been used to create stem cell patterning on polymer substrates [99], to print a single cell type [100] or a precise arrangement of multiple cell types [101].

Extrusion-based bioprinting usually allows the deposition of biological materials layer-by-layer by means of a pneumatic or mechanical extrusion system. This technology permits the deposition of very high cell densities and the fabrication of larger structures at greater speed, at the expense of resolution (200 μm) and cell viability. In general, cell viability has been shown to be lower than inkjet-based bioprinting, due to shear stresses induced by pressure and nozzle gauge [102], although it depends on multiple parameters, such as the material properties and the cell type. Examples of cell-laden tissue constructs developed by using extrusion-based bioprinter included stem cells encapsulated in decellularised extracellular matrix of adipose, cartilage and heart tissues [103], human mesenchymal stem cells to engineer bone and cartilage architectures [104] and embryonic stem cells [97]. To our knowledge, only one study reported in the literature has demonstrated the bioprinting of human cornea epithelial cells using an extrusion-based printer [105]. In this study, 94.6% of cells survived, following extrusion in a collagen/gelatine/alginate-based hydrogel. These cells went on to proliferate and express the cornea epithelial-specific marker cytokeratin 3. Nevertheless, a 3D shape unrepresentative of cornea was printed, suggesting that further studies are required.

In laser-assisted bioprinting, a laser is focused on an absorbing substrate that overlays a layer of biological material. The laser indirectly induces a droplet of the biological material towards a collecting substrate. Laser-assisted bioprinting is advantageous as it avoids clogging and mechanical stresses, thus facilitating high cell viability post-printing. Furthermore, the spatial accuracy is below 5 µm [106]. Despite these advantages, this technique is time-consuming and more costly in comparison to the other strategies. Laser-assisted bioprinting has been used successfully to print layered patterns of human osteoprogenitor cells in 2D and 3D [107], mesenchymal stem cells [108], and multiple cell types simultaneously [109], but has yet to be used for cornea applications.

Stereolithography was the first developed additive manufacturing technique. In this technology, a photo-sensitive material is solidified by means of light. Single or multi-photon methods allow 2D or 3D structures to be printed. A related technique, called two photon polymerization (2PP) is a promising method for 3D nanofabrication, as it allows the generation of complex geometries while precisely controlling scaffold topography and, due to its nanoscale resolution, allows fabrication at a subcellular scale (1–10 µm). The potential of 2PP techniques has begun to show in some recent studies, and has been used in combination with preosteoblast cells [110], adipose stem cells [111], human adipose-derived stem cells, and human bone marrow stem cells [112].

Among the 3D printing techniques investigated, inkjet printing, due to its resolution, high speed and cost-effectiveness, may be suitable for the fabrication of the limbal region and for the recreation of the native microtopography. Extrusion-based printing may be suitable for the deposition of multiple cell types, at a high cell density, and materials to fabricate a layered cornea structure using multiple print-heads. On the contrary, this technique may be inappropriate for fabricating finer microstructures such as the limbus. The high resolution of laser-assisted printing, despite being time consuming, and two photon stereolithography could allow the replication of limbal niches with the incorporation of micropatterns on the material surface to control stem cell fate. For these reasons, these technologies need to be further investigate in this area.

Conclusion

To build functional *in vitro* models or cornea substitutes destined for the clinic, it will be necessary to more

accurately replicate the native tissue structure to build more architecturally and biologically relevant constructs. Current and upcoming techniques, such as those offered by additive manufacturing, are promising for cornea tissue engineering strategies and may aid in the advancement of this research field.

Acknowledgments

We would like to thank the Medical Research Council (MRC)-EPSRC Centre for Doctoral Training (CDT) in Regenerative Medicine (EP/L015072/1) for studentships awarded to E. Prina and P. Mistry, and the European Cooperation in Science and Technology (EU-COST) program BM1302 'Joining Forces in Corneal Regeneration Research' to support the Short Term Scientific Mission (STSM) of E. Prina at Fondazione Banca degli Occhi del Veneto, Italy.

References

1. Gain, P., Jullienne, R., He, Z., et al. (2016). Global Survey of Corneal Transplantation and Eye Banking. *JAMA Ophthalmology*, *134*(2), 167–173.
2. Boisjoly, H. M., Tourigny, R., Bazin, R., et al. (1993). Risk Factors of Corneal Graft Failure. *Ophthalmology*, *100*(11), 1728–1735.
3. Ilari, L., & Daya, S. M. (2002). Long-term outcomes of keratolimbal allograft for the treatment of severe ocular surface disorders. *Ophthalmology*, *109*(7), 1278–1284.
4. Henderson, T. R., Coster, D. J., & Williams, K. A. (2001). The long term outcome of limbal allografts: the search for surviving cells. *The British journal of ophthalmology*, *85*(5), 604–9.
5. Dua, H. S., Faraj, L. a., Said, D. G., Gray, T., & Lowe, J. (2013). Human corneal anatomy redefined: A novel pre-descemet's layer (Dua's Layer). *Ophthalmology*, *120*(9), 1778–1785.
6. Dua, H. S., & Azuara-Blanco, A. (2000). Limbal Stem Cells of the Corneal Epithelium. *Survey of Ophthalmology*, *44*(5), 415–425.
7. Dua, H. S., Shanmuganathan, V. A., Powell-Richards, A. O., Tighe, P. J., & Joseph, A. (2005). Limbal epithelial crypts: a novel anatomical structure and a putative limbal stem cell niche. *The British journal of ophthalmology*, *89*(5), 529–32.
8. Fernandes, M., Sangwan, V. S., Rao, S. K., et al. (2004). Limbal stem cell transplantation. *Indian journal of ophthalmology*, *52*(1), 5–22.
9. Marshall, G. E., Konstas, A. G., & Lee, W. R. (1991). Immunogold Fine-Structural Localization of Extracellular-Matrix Components in Aged Human Cornea .1. Types-I-Iv Collagen and Laminin. *Graefes Archive for Clinical and Experimental Ophthalmology*, *229*(2), 157–163.
10. Scott, J. E., & Thomlinson, a M. (1998). The structure of interfibrillar proteoglycan bridges (shape modules') in extracellular matrix of fibrous connective tissues and their stability in various chemical environments. *Journal of anatomy*, *192*(1998), 391–405.
11. Chakravarti, S., Petroll, W. M., Hassell, J. R., et al. (2000). Corneal opacity in lumican-null mice: defects in collagen fibril structure and packing in the posterior stroma. *Investigative ophthalmology & visual science*, *41*(11), 3365–73.
12. Meek, K. M., & Boote, C. (2004). The organization of collagen in the corneal stroma. *Experimental Eye Research*, *78*(3), 503–512.
13. Poole, C. A., Brookes, N. H., & Clover, G. M. (1993). Keratocyte networks visualised in the living cornea using vital dyes. *Journal of cell science*, 685–91.
14. West-Mays, J. A., & Dwivedi, D. J. (2006). The keratocyte: Corneal stromal cell with variable repair phenotypes. *The International Journal of Biochemistry & Cell Biology*, *38*(10), 1625–1631.
15. Beales, M. P., Funderburgh, J. L., Jester, J. V, & Hassell, J. R. (1999). Proteoglycan synthesis by bovine keratocytes and corneal fibroblasts: maintenance of the keratocyte phenotype in culture. *Investigative ophthalmology & visual science*, *40*(8), 1658–63.
16. Funderburgh, J. L., Mann, M. M., & Funderburgh, M. L. (2003). Keratocyte phenotype mediates proteoglycan structure: A role for fibroblasts in corneal fibrosis. *Journal of Biological Chemistry*, *278*(46), 45629–45637.
17. Jester, J. V, Petroll, W. M., Barry, P. A., & Cavanagh, H. D. (1995). Expression of alpha-smooth muscle (alpha-SM) actin during corneal stromal wound healing. *Investigative ophthalmology & visual science*, *36*(5), 809–19.
18. Helary, C., Ovtracht, L., Coulomb, B., Godeau, G., & Giraud-Guille, M. M. (2006). Dense fibrillar collagen matrices: A model to study myofibroblast behaviour during wound healing. *Biomaterials*, *27*(25), 4443–4452.
19. Hashmani, K., Branch, M., Sidney, L., et al. (2013). Characterization of corneal stromal stem cells with the potential for epithelial transdifferentiation. *Stem Cell Research & Therapy*, *4*(3), 75.
20. Sidney, L. E., Branch, M. J., Dua, H. S., & Hopkinson, A. (2015). Effect of culture medium on propagation and phenotype of corneal stroma–derived stem cells. *Cytotherapy*, *17*(12), 1706–1722.
21. Waring, G. O., Bourne, W. M., Edelhauser, H. F., & Kenyon, K. R. (1982). The corneal endothelium. Normal and pathologic structure and function. *Ophthalmology*, *89*(6), 531–590.
22. Capella, J. A., & Kaufman, H. E. (1969). Human corneal endothelium. *Documenta Ophthalmologica*, *26*(1), 1–8.

23. Lewis, P. N., White, T. L., Young, R. D., et al. (2016). Three-dimensional arrangement of elastic fibers in the human corneal stroma. *Exp Eye Res*, *146*, 43–53.
24. Whitcher, J. P., Srinivasan, M., & Upadhyay, M. P. (2001). Corneal blindness: A global perspective. *Bulletin of the World Health Organization*, *79*(3), 214–221.
25. Dandona, R., & Dandona, L. (2003). Corneal blindness in a southern Indian population: need for health promotion strategies. *The British journal of ophthalmology*, *87*(2), 133–41.
26. Hicks, C. R., Fitton, J. H., Chirila, T. V., Crawford, G. J., & Constable, I. J. (1997). Keratoprostheses: Advancing toward a true artificial cornea. *Survey of Ophthalmology*, *42*(2), 175–189.
27. Chen, C. S., Mrksich, M., Huang, S., Whitesides, G. M., & Ingber, D. E. (1997). Geometric Control of Cell Life and Death, *276*(May), 1425–1428.
28. McNamara, L. E., Burchmore, R., Riehle, M. O., et al. (2012). The role of microtopography in cellular mechanotransduction. *Biomaterials*, *33*(10), 2835–2847.
29. Yim, E. K. F., Darling, E. M., Kulangara, K., Guilak, F., & Leong, K. W. (2010). Nanotopography-induced changes in focal adhesions, cytoskeletal organization, and mechanical properties of human mesenchymal stem cells. *Biomaterials*, *31*(6), 1299–1306.
30. McNamara, L. E., Sjöström, T., Seunarine, K., et al. (2014). Investigation of the limits of nanoscale filopodial interactions. *Journal of tissue engineering*, *5*(JANUARY), 2041731414536177.
31. Yang, J., Rose, F. R. A. J., Gadegaard, N., & Alexander, M. R. (2009). A high-throughput assay of cell-surface interactions using topographical and chemical gradients. *Advanced Materials*, *21*(3), 300–304.
32. Abrams, G. a, Schaus, S. S., Goodman, S. L., Nealey, P. F., & Murphy, C. J. (2000). Nanoscale topography of the corneal epithelial basement membrane and Descemet's membrane of the human. *Cornea*, *19*(1), 57–64.
33. Teixeira, A. I., Abrams, G. A., Bertics, P. J., Murphy, C. J., & Nealey, P. F. (2003). Epithelial contact guidance on well-defined micro- and nanostructured substrates. *Journal of cell science*, *116*(Pt 10), 1881–92.
34. Teixeira, A. I., Abrams, G. A., Murphy, C. J., & Nealey, P. F. (2003). Cell behavior on lithographically defined nanostructured substrates. *Journal of Vacuum Science & Technology B: Microelectronics and Nanometer Structures*, *21*(2), 683.
35. Teixeira, A. I., McKie, G. A., Foley, J. D., et al. (2006). The effect of environmental factors on the response of human corneal epithelial cells to nanoscale substrate topography. *Biomaterials*, *27*(21), 3945–3954.
36. Tocce, E. J., Smirnov, V. K., Kibalov, D. S., et al. (2010). The ability of corneal epithelial cells to recognize high aspect ratio nanostructures. *Biomaterials*, *31*(14), 4064–4072.
37. Evans, M. D. M., McFarland, G. A., Taylor, S., & Walboomers, X. F. (2005). The response of healing corneal epithelium to grooved polymer surfaces. *Biomaterials*, *26*(14), 1703–1711.
38. Fraser, S. A., Ting, Y. H., Mallon, K. S., et al. (2008). Sub-micron and nanoscale feature depth modulates alignment of stromal fibroblasts and corneal epithelial cells in serum-rich and serum-free media. *Journal of Biomedical Materials Research - Part A*, *86*(3), 725–735.
39. Eberwein, P., Steinberg, T., Schulz, S., et al. (2011). Expression of keratinocyte biomarkers is governed by environmental biomechanics. *European Journal of Cell Biology*, *90*(12), 1029–1040.
40. Teo, B. K. K., Goh, K. J., Ng, Z. J., Koo, S., & Yim, E. K. F. (2012). Functional reconstruction of corneal endothelium using nanotopography for tissue-engineering applications. *Acta Biomaterialia*, *8*(8), 2941–2952.
41. Koo, S., Muhammad, R., Peh, G. S. L., Mehta, J. S., & Yim, E. K. F. (2014). Micro- and nanotopography with extracellular matrix coating modulate human corneal endothelial cell behavior. *Acta Biomaterialia*, *10*(5), 1975–1984.
42. Lawrence, B. D., Pan, Z., & Rosenblatt, M. I. (2012). Silk Film Topography Directs Collective Epithelial Cell Migration. *PLoS ONE*, *7*(11).
43. Bray, L. J., George, K. A., Hutmacher, D. W., Chirila, T. V., & Harkin, D. G. (2012). A dual-layer silk fibroin scaffold for reconstructing the human corneal limbus. *Biomaterials*, *33*(13), 3529–3538.
44. Lawrence, B. D., Marchant, J. K., Pindrus, M. A., Omenetto, F. G., & Kaplan, D. L. (2009). Silk film biomaterials for cornea tissue engineering. *Biomaterials*, *30*(7).
45. Gil, E. S., Park, S.-H., Marchant, J., Omenetto, F., & Kaplan, D. L. (2010). Response of Human Corneal Fibroblasts on Silk Film Surface Patterns. *Macromolecular Bioscience*, *10*(6), 664–673.
46. Wu, J., Rnjak-Kovacina, J., Du, Y., et al. (2014). Corneal stromal bioequivalents secreted on patterned silk substrates. *Biomaterials*, *35*(12), 3744–3755.

47. Yanez-Soto, B., Liliensiek, S. J., Gasiorowski, J. Z., Murphy, C. J., & Nealey, P. F. (2013). The influence of substrate topography on the migration of corneal epithelial wound borders. *Biomaterials*, *34*(37), 9244–9251.
48. Vrana, N. E., Elsheikh, A., Builles, N., Damour, O., & Hasirci, V. (2007). Effect of human corneal keratocytes and retinal pigment epithelial cells on the mechanical properties of micropatterned collagen films. *Biomaterials*, *28*(29), 4303–4310.
49. Hackett, J. M., Lagali, N., Merrett, K., et al. (2011). Biosynthetic corneal implants for replacement of pathologic corneal tissue: Performance in a controlled rabbit alkali burn model. *Investigative Ophthalmology and Visual Science*, *52*(2), 651–657.
50. Liu, W., Deng, C., McLaughlin, C. R., et al. (2009). Collagen-phosphorylcholine interpenetrating network hydrogels as corneal substitutes. *Biomaterials*, *30*(8), 1551–1559.
51. Fagerholm, P., Lagali, N. S., Merrett, K., et al. (2010). A biosynthetic alternative to human donor tissue for inducing corneal regeneration: 24-month follow-up of a phase 1 clinical study. *Science translational medicine*, *2*(46), 46ra61.
52. Mirazul Islam, M., Cėpla, V., He, C., et al. (2015). Functional fabrication of recombinant human collagen–phosphorylcholine hydrogels for regenerative medicine applications. *Acta Biomaterialia*, *12*, 70–80.
53. Dua, H. S., Gomes, J. A. P., King, A. J., & Maharajan, V. S. (2004). The amniotic membrane in ophthalmology. *Survey of Ophthalmology*, *49*(1), 51–77.
54. Meller, D., Pires, R. T. F., & Tseng, S. C. G. (2002). Ex vivo preservation and expansion of human limbal epithelial stem cells on amniotic membrane cultures. *The British journal of ophthalmology*, *86*(4), 463–71.
55. Hopkinson, A., McIntosh, R. S., Shanmuganathan, V., Tighe, P. J., & Dua, H. S. (2006). Proteomic analysis of amniotic membrane prepared for human transplantation: Characterization of proteins and clinical implications. *Journal of Proteome Research*, *5*(9), 2226–2235.
56. Rahman, I., Said, D. ., Maharajan, V. ., & Dua, H. . (2009). Amniotic membrane in ophthalmology: indications and limitations. *Eye*, *23*, 1954–61.
57. Chen, B., Jones, R. R., Mi, S., et al. (2012). The mechanical properties of amniotic membrane influence its effect as a biomaterial for ocular surface repair. *Soft Matter*, *8*(32), 8379.
58. Lai, J. Y., Lue, S. J., Cheng, H. Y., & Ma, D. H. K. (2013). Effect of matrix nanostructure on the functionality of carbodiimide cross-linked amniotic membranes as limbal epithelial cell scaffolds. *Journal of Biomedical Nanotechnology*, *9*(12), 2048–2062.
59. Ma, D. H. K., Chen, H. C., Ma, K. S. K., et al. (2016). Preservation of human limbal epithelial progenitor cells on carbodiimide cross-linked amniotic membrane via integrin-linked kinase-mediated Wnt activation. *Acta Biomaterialia*, *31*(259), 144–155.
60. Wang, S., Ghezzi, C. E., Gomes, R., et al. (2017). In vitro 3D corneal tissue model with epithelium, stroma, and innervation. *Biomaterials*, *112*, 1–9.
61. Kolli, S., Lako, M., Figueiredo, F., Mudhar, H., & Ahmad, S. (2008). Loss of corneal epithelial stem cell properties in outgrowths from human limbal explants cultured on intact amniotic membrane. *Regenerative medicine*, *3*(3), 329–42.
62. Ortega, I., Deshpande, P., Gill, A., MacNeil, S., & Claeyssens, F. (2013). Development of a microfabricated artificial limbus with micropockets for cell delivery to the cornea. *Biofabrication*, *5*(2), 25008.
63. Ortega, I., Ryan, A. J., Deshpande, P., MacNeil, S., & Claeyssens, F. (2013). Combined microfabrication and electrospinning to produce 3-D architectures for corneal repair. *Acta biomaterialia*, *9*(3), 5511–20.
64. Ortega, I., McKean, R., Ryan, A. J., MacNeil, S., & Claeyssens, F. (2014). Characterisation and evaluation of the impact of microfabricated pockets on the performance of limbal epithelial stem cells in biodegradable PLGA membranes for corneal regeneration. *Biomaterials Science*, *2*, 723.
65. Foster, J. W., Jones, R. R., Bippes, C. a, Gouveia, R. M., & Connon, C. J. (2014). Differential nuclear expression of Yap in basal epithelial cells across the cornea and substrates of differing stiffness. *Experimental eye research*, *127*, 37–41.
66. Zhao, X., Song, W., Liu, S., & Ren, L. (2016). Corneal regeneration by utilizing collagen based materials. *Science China Chemistry*, *59*(12), 1548–1553.
67. Mi, S., Chen, B., Wright, B., & Connon, C. J. (2010). Plastic compression of a collagen gel forms a much improved scaffold for ocular surface tissue engineering over conventional collagen gels. *Journal of Biomedical Materials Research - Part A*, *95 A*(2), 447–453.
68. Xiao, X., Pan, S., Liu, X., et al. (2014). In vivo study of the biocompatibility of a novel compressed collagen

hydrogel scaffold for artificial corneas. *Journal of Biomedical Materials Research - Part A*, *102*(6), 1782–1787.
69. Alekseeva, T., Hadjipanayi, E., Abou Neel, E. A., & Brown, R. A. (2012). Engineering stable topography in dense bio-mimetic 3D collagen scaffolds. *European Cells and Materials*, *23*, 28–40.
70. Levis, H. J., Brown, R. A., & Daniels, J. T. (2010). Plastic compressed collagen as a biomimetic substrate for human limbal epithelial cell culture. *Biomaterials*, *31*(30), 7726–7737.
71. Levis, H. J., Massie, I., Dziasko, M. a, Kaasi, A., & Daniels, J. T. (2013). Rapid tissue engineering of biomimetic human corneal limbal crypts with 3D niche architecture. *Biomaterials*, *34*(35), 8860–8.
72. Massie, I., Levis, H. J., & Daniels, J. T. (2014). Response of human limbal epithelial cells to wounding on 3D RAFT tissue equivalents: Effect of airlifting and human limbal fibroblasts. *Experimental Eye Research*, *127*.
73. Shortt, A. J., Secker, G. A., Munro, P. M., et al. (2007). Characterization of the Limbal Epithelial Stem Cell Niche: Novel Imaging Techniques Permit In Vivo Observation and Targeted Biopsy of Limbal Epithelial Stem Cells. *Stem Cells*, *25*(6), 1402–1409.
74. Grieve, K., Ghoubay, D., Georgeon, C., Thouvenin, O., & Bouheraoua, N. (2015). Three-dimensional structure of the mammalian limbal stem cell niche. *Experimental Eye Research*, *140*, 75–84.
75. Mishima, S., Gasset, A., Klyce, S. D., JL, B., & Baum, J. L. (1966). Determination of tear volume and tear flow. *Investigative ophthalmology*, *5*(3), 264–276.
76. Furukawa, R. E., & Polse, K. A. (1978). Changes in tear flow accompanying aging. *American journal of optometry and physiological optics*, *55*(2), 69–74.
77. Mohammadi, S., Postnikoff, C., Wright, A. M., & Gorbet, M. (2014). Design and development of an in vitro tear replenishment system. *Annals of Biomedical Engineering*, *42*(9), 1923–1931.
78. Bajgrowicz, M., Phan, C. M., Subbaraman, L. N., & Jones, L. (2015). Release of ciprofloxacin and moxifloxacin from daily disposable contact lenses from an in vitro eye model. *Investigative Ophthalmology and Visual Science*, *56*(4), 2234–2242.
79. Phan, C.-M., Bajgrowicz, M., Gao, H., Subbaraman, L., & Jones, L. W. (2016). Release of Fluconazole from Contact Lenses Using a Novel In Vitro Eye Model. *Optometry and Vision Science*, *93*(4), 387–394.
80. Karns, K., & Herr, A. E. (2011). Human tear protein analysis enabled by an alkaline microfluidic homogeneous immunoassay. *Analytical Chemistry*, *83*(21), 8115–8122.
81. Mann, A. M., & Tighe, B. J. (2007). Tear analysis and lens-tear interactions. Part I. Protein fingerprinting with microfluidic technology. *Contact Lens and Anterior Eye*, *30*(3), 163–173.
82. Guan, A., Wang, Y., Phillips, K. S., & Li, Z. (2016). A contact-lens-on-a-chip companion diagnostic tool for personalized medicine. *Lab on a chip*, *16*(7), 1152–1156.
83. Pretor, S., Bartels, J., Lorenz, T., et al. (2015). Cellular Uptake of Coumarin-6 under Microfluidic Conditions into HCE-T Cells from Nanoscale Formulations. *Molecular Pharmaceutics*, *12*(1), 34–45.
84. Sullivan, D. (2002). Proceedings of the 3rd International Conference on the Lacrimal Gland, Tear Film, and Dry Eye Syndromes: Basic Science and Clinical Relevance. November 15-18, 2000, Maui, Hawaii. *Advances in experimental medicine and biology*, *506*(Pt B), 729–1385.
85. Kang, Y. G., Shin, J. W., Park, S. H., et al. (2014). Effects of flow-induced shear stress on limbal epithelial stem cell growth and enrichment. *PLoS ONE*, *9*(3), 1–7.
86. Jin, G., Yang, G. H., & Kim, G. (2015). Tissue engineering bioreactor systems for applying physical and electrical stimulations to cells. *Journal of Biomedical Materials Research - Part B Applied Biomaterials*, *103*(4), 935–948.
87. Puleo, C. M., McIntosh Ambrose, W., Takezawa, T., Elisseeff, J., & Wang, T.-H. (2009). Integration and application of vitrified collagen in multilayered microfluidic devices for corneal microtissue culture. *Lab on a Chip*, *9*(22), 3221.
88. Winkler, M., Simon, M. G., Vu, T., et al. (2014). A microfabricated, optically accessible device to study the effects of mechanical cues on collagen fiber organization. *Biomedical Microdevices*, *16*(2), 255–267.
89. Aghamohammadzadeh, H., Newton, R. H., & Meek, K. M. (2004). X-Ray Scattering Used to Map the Preferred Collagen Orientation in the Human Cornea and Limbus. *Structure*, *12*(2), 249–256.
90. Farrell, R. A., & McCally, R. L. (2000). Corneal transparency. In D. M. Albert & F. A. Jakobiec (Eds.), *Principles and Practice of Ophthalmology* (pp. 629–643). Philadelphia: WB Saunders Company.
91. Meek, K. M., Leonard, D. W., Connon, C. J., Dennis, S., & Khan, S. (2003). Transparency, swelling and scarring in the corneal stroma. *Eye*, *17*(8), 927–936.
92. Barnes, R., Shahin, Y., Gohil, R., & Chetter, I. (2014). Electrical stimulation vs. standard care for chronic

ulcer healing: A systematic review and meta-analysis of randomised controlled trials. *European Journal of Clinical Investigation*, *44*(4), 429–440.
93. Rajnicek, A. M., Foubister, L. E., & McCaig, C. D. (2008). Alignment of corneal and lens epithelial cells by co-operative effects of substratum topography and DC electric fields. *Biomaterials*, *29*(13), 2082–2095.
94. Gao, J., Raghunathan, V. K., Reid, B., et al. (2015). Biomimetic stochastic topography and electric fields synergistically enhance directional migration of corneal epithelial cells in a MMP-3-dependent manner. *Acta Biomaterialia*, *12*(1), 102–112.
95. Zhao, S., Zhu, K., Zhang, Y., et al. (2014). ElectroTaxis-on-a-Chip (ETC): an integrated quantitative high-throughput screening platform for electrical field-directed cell migration. *Lab on a chip*, *14*(22), 4398–4405.
96. Klebe, S., Coster, D. J., & Williams, K. A. (2009). Rejection and acceptance of corneal allografts. *Current Opinion in Organ Transplantation*, *14*(1), 4–9.
97. Ouyang, L., Yao, R., Mao, S., et al. (2015). Three-dimensional bioprinting of embryonic stem cells directs highly uniform embryoid body formation. *Biofabrication*, *7*(4), 44101.
98. Gibson, I., Rosen, D. W., & Stucker, B. (2010). *Additive Manufacturing Technologies*. *Development*. Boston, MA: Springer US.
99. Kim, J. D., Choi, J. S., Kim, B. S., Chan Choi, Y., & Cho, Y. W. (2010). Piezoelectric inkjet printing of polymers: Stem cell patterning on polymer substrates. *Polymer*, *51*(10), 2147–2154.
100. Xu, T., Jin, J., Gregory, C., Hickman, J. J., & Boland, T. (2005). Inkjet printing of viable mammalian cells. *Biomaterials*, *26*(1), 93–99.
101. Xu, T., Zhao, W. X., Zhu, J. M., et al. (2013). Complex heterogeneous tissue constructs containing multiple cell types prepared by inkjet printing technology. *Biomaterials*, *34*(1), 130–139.
102. Chang, R., Nam, J., & Sun, W. (2008). Effects of Dispensing Pressure and Nozzle Diameter on Cell Survival from Solid Freeform Fabrication–Based Direct Cell Writing. *Tissue Engineering Part A*, *14*(1), 41–48.
103. Pati, F., Jang, J., Ha, D.-H., et al. (2014). Printing three-dimensional tissue analogues with decellularized extracellular matrix bioink. *Nature communications*, *5*, 3935.
104. Armstrong, J. P. K., Burke, M., Carter, B. M., Davis, S. A., & Perriman, A. W. (2016). 3D Bioprinting Using a Templated Porous Bioink. *Advanced Healthcare Materials*, *5*(14), 1724–1730.
105. Wu, Z., Su, X., Xu, Y., et al. (2016). Bioprinting three-dimensional cell-laden tissue constructs with controllable degradation. *Scientific reports*, *6*, 24474.
106. Barron, J. A., Wu, P., Ladouceur, H. D., & Ringeisen, B. R. (2004). Biological laser printing: A novel technique for creating heterogeneous 3-dimensional cell patterns. *Biomedical Microdevices*, *6*(2), 139–147.
107. Catros, S., Fricain, J.-C., Guillotin, B., et al. (2011). Laser-assisted bioprinting for creating on-demand patterns of human osteoprogenitor cells and nano-hydroxyapatite. *Biofabrication*, *3*, 25001.
108. Ali, M., Pages, E., Ducom, A., Fontaine, A., & Guillemot, F. (2014). Controlling laser-induced jet formation for bioprinting mesenchymal stem cells with high viability and high resolution. *Biofabrication*, *6*(4), 45001.
109. Gruene, M., Pflaum, M., Hess, C., et al. (2011). Laser Printing of Three-Dimensional Multicellular Arrays for Studies of Cell–Cell and Cell–Environment Interactions. *Tissue Engineering Part C: Methods*, *17*(10), 973–982.
110. Markovic, M., Van Hoorick, J., Hölzl, K., et al. (2015). Hybrid Tissue Engineering Scaffolds by Combination of Three-Dimensional Printing and Cell Photoencapsulation. *Journal of nanotechnology in engineering and medicine*, *6*(2), 0210011–0210017.
111. Silva, K. R., Rezende, R. A., Pereira, F. D. A. S., et al. (2016). Delivery of human adipose stem cells spheroids into lockyballs. *PLoS ONE*, *11*(11), 1–14.
112. Koroleva, A., Deiwick, A., Nguyen, A., et al. (2015). Osteogenic differentiation of human mesenchymal stem cells in 3-D Zr-Si organic-inorganic scaffolds produced by two-photon polymerization technique. *PloS one*, *10*(2), 1–18.

Legend to figures

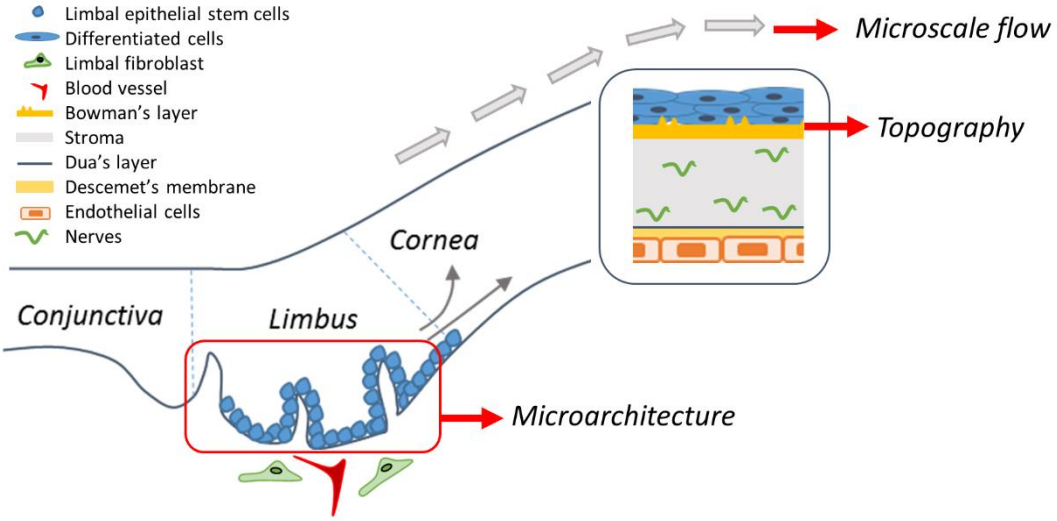

Fig.1: Schematic representation of the cornea, including the limbus. The red arrows indicate the three aspects of corneal bioengineering explored in this review.

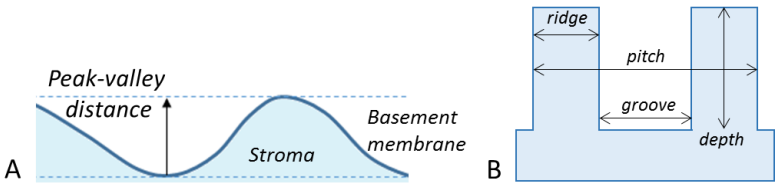

Fig.2: A) Representation of basement membrane, adapted from [32]; B) Surface pattern replicated by Teixeira et al. [35].

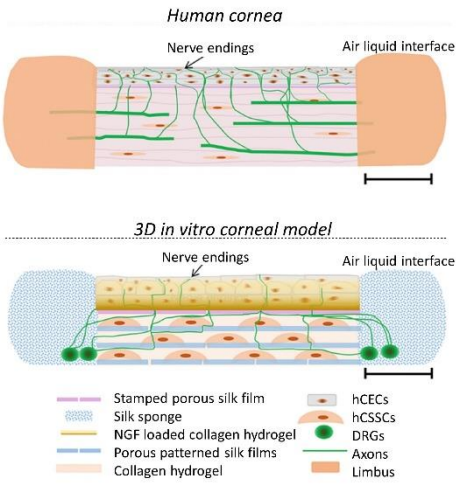

Fig.3: Model developed by Wang et al. [60] (with permission of Elsevier).

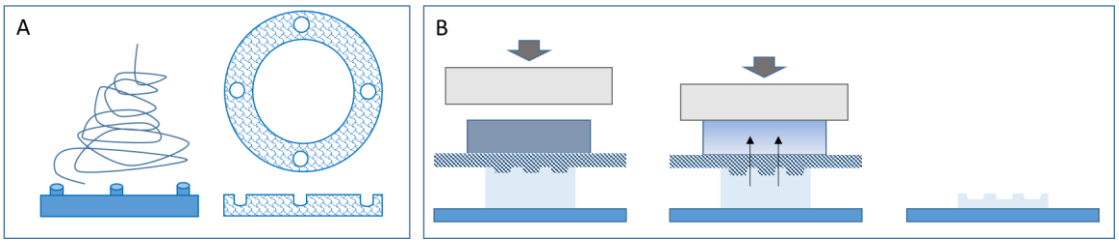

Fig.4: Representation of the techniques used to develop cornea carriers for tissue engineering applications with the insertion of a protective limbus microarchitecture. A) The combination of stereolithography and electrospinning techniques were used to reproduce scaffolds with microfabricated pockets [63]. B) RAFT technique for the development of bioengineered limbal crypts in a collagen construct [71].